Journal of Physics: Conference Series

PAPER • **OPEN ACCESS**

First comparison of LES of an offshore wind turbine wake with dual-Doppler lidar measurements in a German offshore wind farm

To cite this article: L Vollmer *et al* 2015 *J. Phys.: Conf. Ser.* **625** 012001

First comparison of LES of an offshore wind turbine wake with dual-Doppler lidar measurements in a German offshore wind farm

L Vollmer[1], M van Dooren[1], D Trabucchi[1], J Schneemann[1], G Steinfeld[1], B Witha[1], J Trujillo[1] and M Kühn[1]

[1] ForWind, Carl von Ossietzky Universität Oldenburg, Ammerländer Heerstr.136, Oldenburg, DE

E-mail: `lukas.vollmer@forwind.de`

Abstract. Large-Eddy Simulations (LES) are more and more used for simulating wind turbine wakes as they resolve the atmospheric as well as the wake turbulence. Considering the expenses and sparsity of offshore measurements, LES can provide valuable insights into the flow field in offshore wind farms. However, for an application of LES wind fields to assess offshore wind farm flow, a proper validation with measured data is necessary. Such a proper validation requires that the LES can closely reproduce the atmospheric conditions during the measurement. For this purpose, a representation of the large-scale features that drive the wind flow is required. Large-scale-forcing and nudging of the LES model PALM is tested with reanalysis data of the COSMO-DE model for a case study during one particular day in the beginning of 2014 at a German offshore wind farm. As wind and temperature profiles of the LES prove to follow the large-scale features closely, the wake of a single wind turbine is simulated with an advanced version of an actuator disc model. Measurement data is provided by processed dual-Doppler lidar measurements during the same day in the same wind farm. Several methods have been investigated at the University of Oldenburg to compare LES wind fields and lidar measurements. In this study a dual-Doppler algorithm was applied in order to estimate the horizontal stationary wind field. The raw data originate from Plan Position Indicator (PPI) measurements, which have been performed with two long-range wind lidars installed at different opposing platforms at the border of the wind farm.

1. Introduction

The planning of offshore wind farms is still tainted with high risks due to unknown power losses and a higher level of fatigue loads related to wake effects. Thus, a good knowledge of the atmospheric boundary layer and its interaction with the wake flow is essential to predict wind farm power production as well as structural loads on the wind turbines. In recent years, Large-Eddy Simulations (LES) have become a common tool to simulate the influence of atmospheric turbulence on the turbine structure [1, 2] and to study the wakes inside wind farms [3, 4]. In general, measurements do not provide the information necessary for the setup of LES to create comparable atmospheric conditions. So in practice, LES are conducted for idealized situations and are normalized for comparison with results from measurement campaigns. This procedure naturally has several shortcomings. One of them is, that the scale and magnitude of turbulence influenced by e.g. atmospheric stability and the local topographic features at the turbine site are

Journal of Physics: Conference Series **625** (2015) 012001 doi:10.1088/1742-6596/625/1/012001

expected to have significant influence on shape and magnitude of the wake and on the turbine performance [5, 6]. Recently, efforts have been made to establish more realistic conditions [7] in LES or to focus on short-term phenomena like gusts [8].

In the presented study we introduce an approach to establish LES with closely comparable conditions to the atmospheric state recorded during a lidar measurement campaign of wind turbine wakes at the German offshore wind farm *alpha ventus* that is situated approximately 45 km north of the German island Borkum in the North Sea. The lidar measurements provide the rare possibility to have access to wake wind fields from an offshore location. To establish the atmospheric conditions in the model, the variables of the LES are forced towards the state of a COSMO-DE [9] reanalysis. In so doing, meso-scale mean wind and temperature fluctuations are object of the LES. The large distance of the wind farm to the coast should further improve the comparability of the LES with measured conditions as influences of topography and land use can be neglected. The LES wind field is generated for one particular day in the beginning of 2014 and is used for a simulation of a single turbine of the wind farm. Wake velocities from the LES are compared to horizontal wind fields behind the same turbine that were computed from lidar measurements, taken during the same time interval.

We start this paper with an introduction to the lidar data that is used for comparison. In the following, the measured wind data from a met mast close to the wind farm site is compared to the reanalysis data that is used for the large-scale-forcing of the LES. In the last part, the LES using a turbine model is presented and compared to results from the lidar campaign.

2. Measurement scenario

The basis for this study is a lidar measurement campaign that took place during the period from August 2013 until March 2014 at the German offshore wind farm *alpha ventus*. During the campaign three long-range lidars were positioned around the wind farm. Two of the systems were placed on the met mast (FINO1) support platform to the west of the wind farm, the third one was placed on the transformer platform in the south-east corner (see Fig.1). Line-of-sight velocities from PPI (Plan Position Indicator) scans from two of the pulsed lidars were combined to evaluate the horizontal velocity components u and v in a well defined control volume inside the wind farm. The algorithm used is the Multiple-lidar Wind Field Evaluation Algorithm (MuLiWEA), developed at ForWind. The approach is based on a wind vector evaluation on a Cartesian grid and has an adjustment imposed by the continuity equation. For more information the reader is referred to [10].

The setup of the lidar system in *alpha ventus* has some consequences for the measurements. Hard targets in the wind farm, e.g. masts and the wind turbines themselves obstruct the view

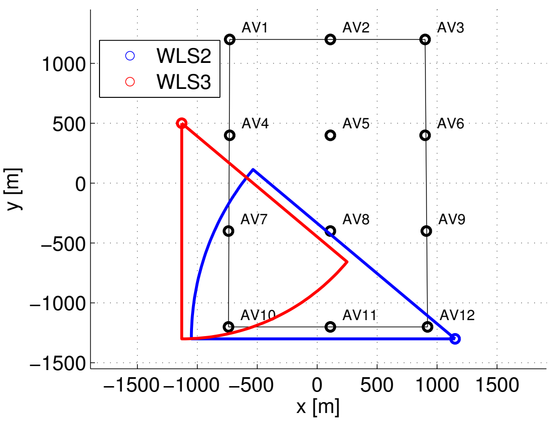

Figure 1. Layout of alpha ventus and position of the two lidars (WLS2, WLS3) that were used for the analysis and the scan area for measurements of the wake of AV10.

of the lidars. The optimal accuracy of the algorithm is reached when scanning under a relative angle of 90° between the individual scans, e.g. scanning the wake of AV3 or AV10. On the other hand the large error at a relative angle of 180° causes that the wake of e.g. AV8 cannot be characterized with sufficient accuracy. Results shown in this study are from selected cases measured at 20 February 2014 behind turbine AV10. The wakes are calculated at hub height of the wind turbine. Only fields that contain enough measurements within a reasonable altitude range centered around hub height are used. In addition, measurements are filtered at both sides of the Carrier-to-Noise level. That means highly scattered signals with a high noise level and reflexions from hard targets, that produce a very high signal, are removed. Velocities are averaged on $(20\ \mathrm{m})^3$ cubes with the center at hub height and over a time interval of 10 min to have more measurements for the calculation of the hub height velocities. Both lidars scan at a relatively small azimuth angle, so 5-7 sweeps over the scan area contribute to the calculation of 10 min mean velocities.

3. Modeling the selected case

3.1. Large-scale-forcing routines

For the modeling of the scenario on 20 February 2014, the LES model PALM was used with the default numeric routines of version 4.0 [11, 12]. The goal of the large-scale-forcing routines is to force the horizontal mean variables of the model towards a time-dependent predefined state. The forcing is done in PALM in two different ways: The first is by a variation of the boundary conditions and the second is by nudging. The time-dependent, large-scale pressure gradients that drive the flow in the model are given by prescribing the vertical profile of the geostrophic wind vector $\vec{v}_g(t)$ for each time step. In addition, the change of potential temperature Θ by horizontal advection is prescribed:

$$\frac{\partial \Theta(z)}{\partial t}|_{LS} = -\left(u(z)_{LS}\frac{\partial \Theta(z)_{LS}}{\partial x} + v(z)_{LS}\frac{\partial \Theta(z)_{LS}}{\partial y}\right)$$

Terms with the subscript $_{LS}$ are the large-scale values of the variables. The change of temperature by horizontal advection acts as a steady sink or source of heat at every grid point of the model. At the lower boundary the bottom temperature, pressure and heat flux is provided by the large-scale-forcing during the simulation .

The term nudging describes a relaxation of the spatial mean LES state $< \phi >$ towards a prescribed state ϕ_{LS} by a time constant τ at every time step.

$$\frac{\partial \phi(z)}{\partial t}|_{Nudge} = -\frac{< \phi(z) > - \phi(z)_{LS}}{\tau}$$

Profiles for the large-scale variables can be set at discrete times and on its own vertical grid. The input is afterwards linearly interpolated on the PALM model vertical grid and on the discrete time steps of the simulation.

3.2. Input data

The forcing input data was taken from a reanalysis with the COSMO-DE model. It is available on a $2.8\,\mathrm{km} \times 2.8\,\mathrm{km}$ horizontal grid and a non-equidistant vertical grid. Instantaneous values of the first order variables are available once per hour. Higher order terms like the surface heat flux are output as an hourly mean. The necessary variables were averaged horizontally over an area of approximately $(120\,\mathrm{km})^2$ around *alpha ventus* to get the large-scale-forcing input for the LES (see Fig.2).

To evaluate the accuracy of the input data, it was compared to measurements at the met mast FINO1. For the predominant south-west wind direction during the scenario, these measurements

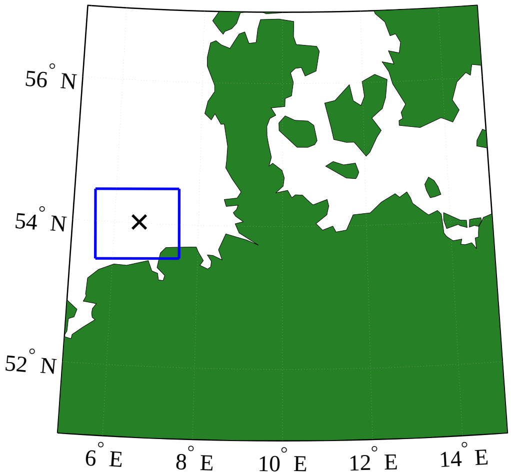

Figure 2. Position of FINO1 (cross) and averaging domain of the COSMO-DE data (box).

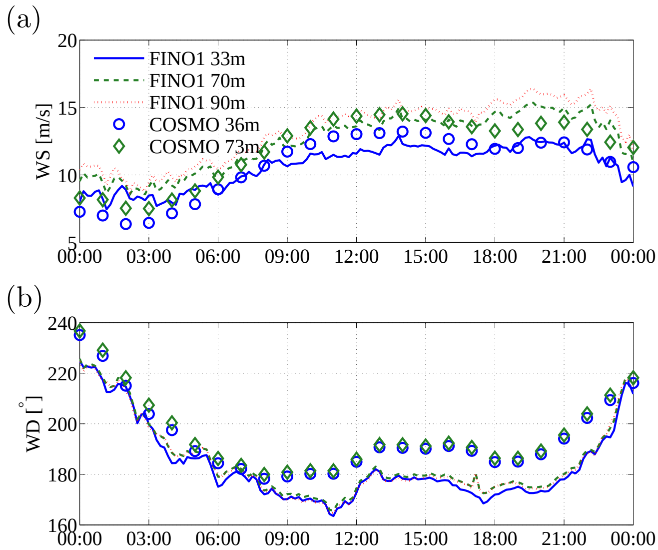

Figure 3. Time series of the wind speed (a) and the wind direction (b) at different heights from FINO1 measurements (lines) and from spatially averaged COSMO-DE data (circles) for 20 February 2014.

are not affected by the adjacent wind farm. 10 min wind speeds from anemometers and wind directions from wind vanes are available for this day at heights of 33 m, 50 m, 60 m, 70 m and 90 m, temperature data is unfortunately not available.

The comparison of the FINO1 measurements with the spatially averaged COSMO-DE data for 20 February 2014 shows some good agreement, especially between the wind measurements at 70 m height and the meso-scale data at 73 m height (see Fig.3). The general trend of wind speed during the day is a speed up from around 8 m/s to 14 m/s from the early morning to noon and a constant strong wind afterwards. The wind direction turns only slightly from south-west to south during the morning and back towards south-west in the evening. There seems to be a quite constant offset of about 10 degrees between the wind direction of the two data sets. Differences are largest for southerly wind during day time. However for this wind direction an influence of *alpha ventus* on the FINO1 measurements can not be ruled out.

3.3. Results from the LES with large-scale-forcing and nudging

The forcing with meso-scale data was tested in PALM for a horizontal and vertical resolution of 5 m. The domain size was 3200 m x 3200 m horizontally and 2200 m vertically with cyclic lateral boundary conditions. At the lower boundary, Monin-Obhukhov similarity theory was applied between the surface and the first grid level. A roughness length of $z_0 = 2 \cdot 10^{-3}$ m was used, corresponding to offshore conditions. Before the forcing was applied, a spin-up period of 6 hours was conducted for atmospheric turbulence to evolve. The process was triggered with random perturbations of the velocity field during the initial phase of the simulation. Initial profiles were the meso-scale profiles at 20 February 2014 0:00 am. After the 6 hour spin up, the time dependent nudging and large-scale-forcing were applied. The relaxation time τ for the nudging of the horizontal velocities and the potential temperature was set to $\tau = 1.5$ h.

Domain-averaged vertical profiles of the PALM output and the forcing profiles are shown in Fig.4. The difference for the initial profile at 0:00 am is caused by the divergence of the wind field during the spin-up before the actual forcing is applied. Afterwards the profiles of the

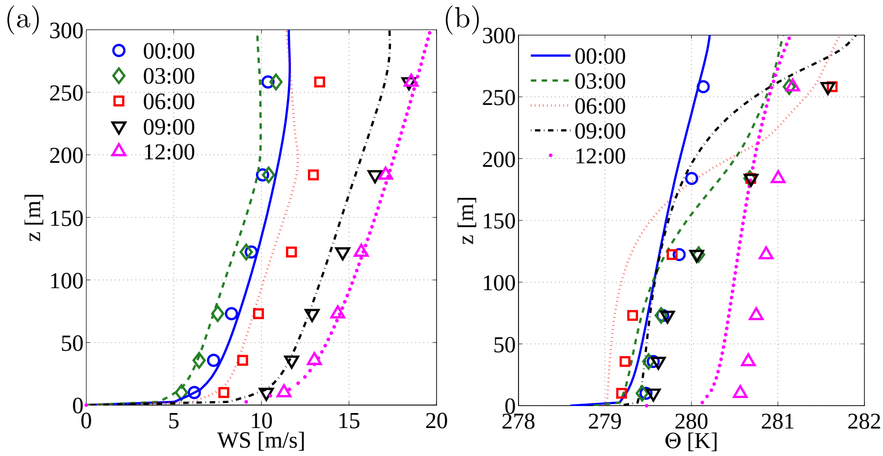

Figure 4. Vertical profiles of wind speed (a) and potential temperature (b) of the COSMO-DE input data (symbols) and the PALM output (lines) during the first 12 h of the large-scale-forcing of the model

LES are close to the forcing data. For the potential temperature a vertically constant offset of about 0.25 K persists. Overall the differences between the LES velocities and the COSMO-DE velocities are small compared to the differences between FINO1 and COSMO-DE.

4. Wind turbine simulation

A LES utilizing a wind turbine model was conducted for the time between 5.30 am and 7.00 am. For this time-span multiple 2D wakes from the lidar-campaign exist for comparison, and furthermore the wind profile of the meso-scale data and of the LES simulation are quite close to the measured profile from the met mast evaluation. The setup was the same as in the aforementioned simulation. Using cyclic boundaries in wake simulations often modifies the results as the wake reenters the boundary and modifies the inflow. In the presented case this effect is attenuated by the slight diagonal inflow, so that the wake is advected through the domain multiple times and vanishes before serving as inflow for the turbine again. As wind turbine model a modified actuator disc model (ADMR) was used that includes non-uniform thrust, a rotational component of the wake and yawing of the turbine. The influence of tower and nacelle on the flow were represented by constant drag coefficients. Further details con be found in [13].

The ADMR is based on blade element momentum theory and requires information about the structure and the lift- and drag coefficients for the different airfoils of the turbine blade. As this information is not available for the turbine AV10, properties of the freely available NREL 5MW turbine of approximately the same size and rated power were used as replacement. To control the rotational speed of the rotor and to maximize power capture below the rated operation point, the generator torque was adjusted for every time step of the simulation (approximately every 0.3 s). The low-pass filtered generator speed was used as the only feedback input, as explained in the turbine definition [14]. Average data was recorded for each 10 min interval starting at 5:40 am. The yaw alignment of the turbine was corrected at the beginning of each interval to the mean wind direction during the interval.

Fig.5 shows the horizontal velocity at hub height for three different time intervals of the LES and the lidar measurements. Velocities from the LES were averaged on $(20\ \mathrm{m})^3$ cubes for better comparison. Results show particularly good agreement in the direction of the wake propagation, indicating that the large-scale-forcing of the LES model delivers a quite accurate wind direction. The magnitude of the wind speed is normalized by the domain averaged wind speed in case of the LES and by the average wind speed measured at 90 m height at FINO1 in case of the lidar measurements. Deviations from unity outside of the wake are probably due to the nonhomogeneity of the wind field during the short averaging interval and due to the

Journal of Physics: Conference Series **625** (2015) 012001 doi:10.1088/1742-6596/625/1/012001

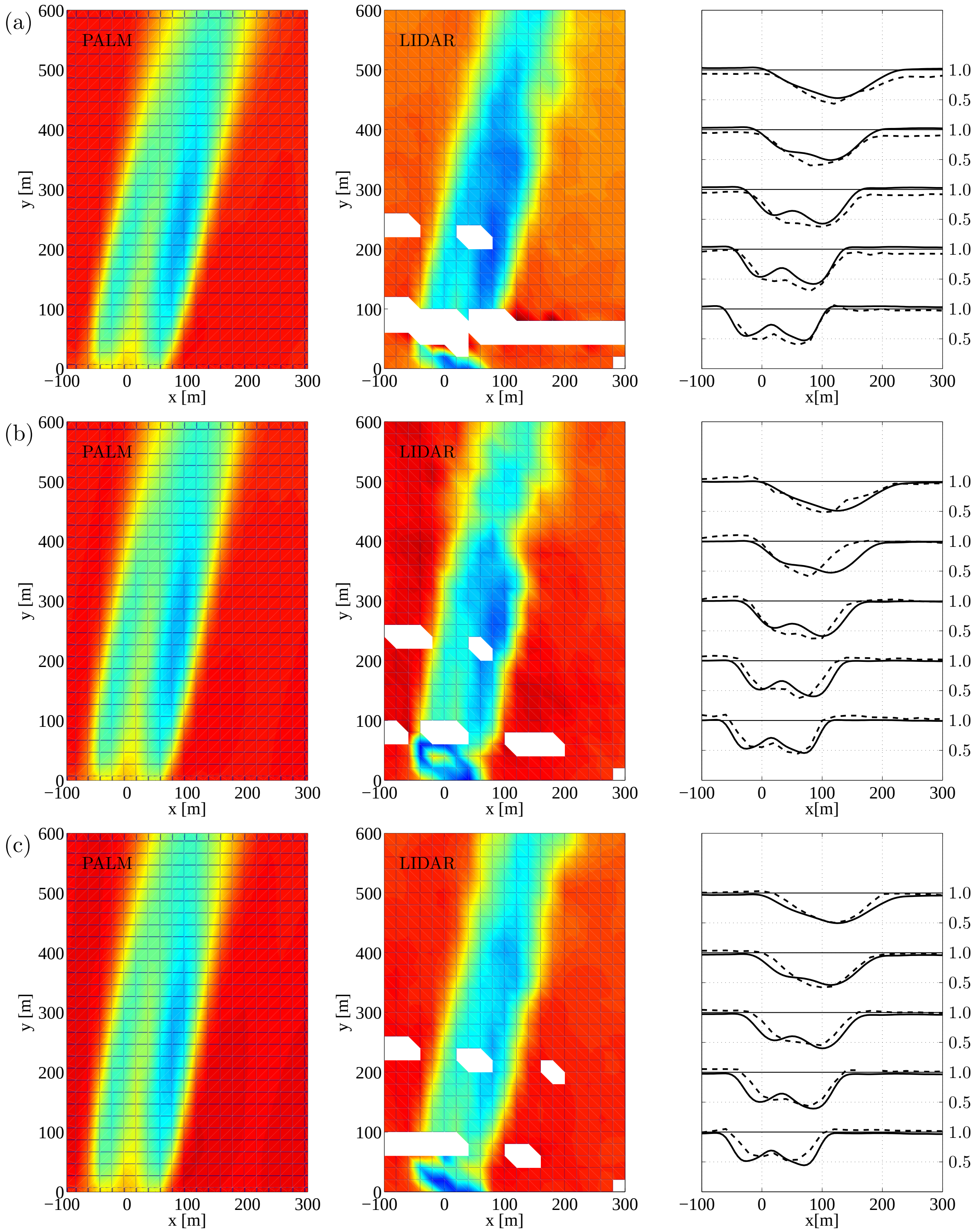

Figure 5. Hub height wind speed during three different 10 min measurement and simulation intervals starting at (a) 5:40 am, (b) 6:10 am and (c) 6:30 am. In the rightmost panels cross-sections of PALM wind speed (solid lines) and measured wind speed (dashed lines) at different distances are compared. Wind speeds of simulations and measurements are normalized by the domain-averaged wind speed at hub height and by the 10 min average wind speed at 90 m measured at FINO1, respectively.

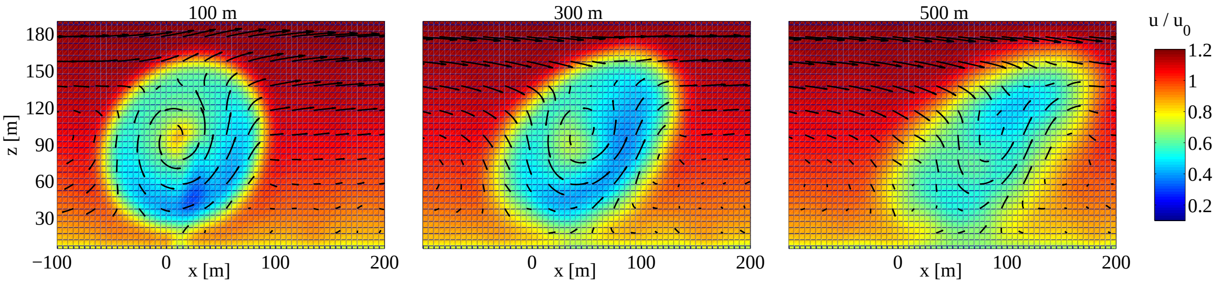

Figure 6. Streamwise (contours) and cross stream component (vectors) of the normalized simulated wind speed at different distances behind the wind turbine for the interval starting at 6:30 am.

distance of the met mast to AV10 (see Fig.1). The deficit is generally slightly larger in the lidar measurements. Both results show a development from a double Gaussian-shaped deficit to a single Gaussian-shaped deficit in the first 500 m downstream of the wind turbine. The double Gaussian shape is more pronounced and the transition appears to occur further downstream in the LES. A clearly visible feature of the wakes is the higher deficit on the right side of the wake, where the clockwise rotation of the rotor causes an upward flow. This upward flow advects lower momentum due to the vertical shear of the wind field. The effect is more clear in the vertical cross sections shown in Fig.6, where also the impact of the vertical wind veer on the shape of the wake is evident.

5. Discussion

In the scope of this paper we show that the LES model PALM delivers realistic results, when driven by large-scale profiles from a COSMO-DE reanalysis using the implemented large-scale-forcing and nudging routines. As base for comparison, wind data from the FINO1 met mast was used. The diurnal cycle of wind speed and direction measured during one particular day of operation was quite well reproduced with the model. The modeled wind field was subsequently used for a LES study with a wind turbine model. Results from the simulation were compared to horizontal wind fields computed from lidar wake measurements, that were taken at the exact same time. We find that in particular the wind direction and thus the propagation of the wake is well reproduced in the model. Furthermore wind turbine wakes from the lidar measurements and the LES show the same characteristic features, even though the turbines were not exactly the same. This encourages to continue working with the wind turbine model as well as with the usage of the large-scale forcing routines.

For further use, the sensitivity to the relaxation time constant of the nudging procedure and the procedure to develop initial turbulence before starting the forcing needs to be evaluated in more detail. Also the capability of the LES to develop realistic atmospheric turbulence, when forced towards an external state, needs further evaluation.

As manner to compare LES results with lidar measurements the recently developed dual-Doppler algorithm MuLiWEA, that combines two long-range lidar measurements to estimate a stationary 2D wind field, was used. This approach is quite intuitive as a realization for averaged measurements because the differences are well visible. Other methods are also studied at ForWind, e.g. a direct comparison of line-of-sight velocities with projected LES velocities, that allows for a more detailed evaluation of atmospheric and wake turbulence.

Acknowledgments

The work presented in this study is funded by the national research projects CompactWind and Parallelrechner-Cluster für CFD und WEA-Modellierung (FKZ 0325492B, 0325220; Federal Ministry for Economic Affairs and Energy) and the Ministry for Education, Science and Culture of Lower Saxony. Computer resources have been partly provided by the North German Supercomputing Alliance (HLRN). We thank Deutscher Wetterdienst (DWD) for providing analysis data. The authors further thank R. Heinze from IMUK Hannover for assistance on the execution and preparation of the large-scale-forcing routines of the LES model PALM.

References

[1] Lee S, Churchfield M J, Moriarty P J, Jonkman J and Michalakes J 2013 *J. Sol. Energy Eng.* **135** doi: 10.1115/1.4023319
[2] Park J, Basu S and Manuel L 2013 *Wind Energy* **17** 359–385 doi: 10.1002/we.1580
[3] Lu H and Porté-Agel F 2011 *Phys. Fluids* **23** 065101 doi: 10.1063/1.3589857
[4] Witha B, Steinfeld G, Dörenkämper M and Heinemann D 2014 *J. Phys.: Conference Series* **555** 012108 doi: 10.1088/1742-6596/555/1/012108
[5] Wharton S and Lundquist J K 2010 Tech. Rep. LLNL-TR-424425 Lawrence Livermore National Laboratory
[6] Dörenkämper M, Tambke J, Steinfeld G, Heinemann D and Kühn M 2014 *J. Phys.: Conference Series* **555** 012029 doi: 10.1088/1742-6596/555/1/012029
[7] Lundquist J K, Mirocha J D and Kosovic B 2010 *The 5th Int. Symp. on Computational Wind Engineering, Chapel Hill, North Carolina, USA*
[8] Storey R, Norris S and Cater J 2013 *Proc. of the World Congress on Engineering 2013 Vol III, WCE 2013, July 3 - 5, 2013, London, U.K.*
[9] Baldauf M, Förstner J, Klink S, Reinhardt T, Schraff C, Seifert A, Stephan K and Wetterdienst D 2009 *Deutscher Wetterdienst, Geschäftsbereich Forschung und Entwicklung, Offenbach, Germany*
[10] v Dooren M 2014 Master's thesis ForWind - University of Oldenburg
[11] Raasch S and Schröter M 2001 *Meteorol. Z.* **10** 363–372 doi: 10.1127/0941-2948/2001/0010-0363
[12] Maronga B, Gryschka M, Heinze R, Hoffmann F, Kanani-Sühring F, Keck M, Ketelsen K, Letzel M O, Sühring M and Raasch S 2015 *Geosci. Model Dev. Discuss.* **8** 1539–1637 doi: 10.5194/gmdd-8-1539-2015
[13] Dörenkämper M, Witha B, Steinfeld G, Heinemann D and Kühn M 2015 *J. Wind Eng. Ind. Aerod.* accepted for publication doi : 10.1016/j.jweia.2014.12.011
[14] Jonkman J M, Butterfield S, Musial W and Scott G 2009 Technical Report NREL/TP-500-38060 National Renewable Energy Laboratory